# Resolving the Vergence-Accommodation Conflict in Head Mounted Displays

## A review of problem assessments, potential solutions, and evaluation methods

### Gregory Kramida and Amitabh Varshney

**Abstract**—The vergence-accommodation conflict remains a major problem in head-mounted displays for virtual and augmented reality (VR and AR). In this review, we discuss why this problem is pivotal for nearby tasks in VR and AR, present a comprehensive classification of potential solutions, along with advantages and shortfalls of each category, and briefly describe various methods that can be used to better evaluate the solutions.

**Index Terms**—Vergence-Accommodation Conflict, Head-Mounted Displays

✦

## 1 INTRODUCTION

The vergence-accommodation conflict (henceforth referred to as VAC), also known as accommodation-convergence mismatch, is a well-known problem in the realm of head(or helmet)-mounted displays (HMDs), also referred to as head-worn displays (HWDs) [1], and stereoscopic displays in general: it forces the viewer's brain to unnaturally adapt to conflicting cues and increases fusion time of binocular imagery, while decreasing fusion accuracy [2]. This contributes to (sometimes severe) visual fatigue (asthenopia), especially during prolonged use [3], [4], [5], which, for some people, can even cause serious side-effects long after cessation of using the device [6].

The current work is a checkpoint of the current state of the VAC problem as it relates to HMDs for augmented reality (AR) and virtual reality (VR), and a comprehensive listing and discussion of potential solutions. With this review, we intend to provide solid informational foundations on how address VAC for any researcher working on or with HMD displays, whether they are working on new solutions to the problem specifically, or designing a prototype for a related application.

In the remainder of this section we present a review of publications assessing the nature of the VAC problem and discussing its severity and importance within different contexts. In the following Section 2, comprising the bulk of this review, we discuss the various display designs that attempt to solve the problem, addressing the advantages and shortfalls of each, as well as related technology which could potentially

help with this issue in future designs. In Section 3, we describe the various methods and metrics that have been proposed or applied to evaluate the effectiveness of existing solutions. Finally, in Section 4, we identify potential areas within the solution space that have yet to be explored or can be improved.

### 1.1 The Accommodation-Vergence Conflict

The human visual system employs multiple depth stimuli, a more complete classification of which can be found in a survey by Reichelt et al. [5]. The same survey finds that occulomotor cues of consistent vergence and accommodation, which are, in turn, related to retinal cues of blur and disparity, are critical to comfortable 3D viewing experience. Retinal blur is the actual visual cue driving the occulomotor response of accommodation, or adjustment of the eye's lens to focus on the desired depth, thus minimizing the blur. Likewise, retinal disparity is the visual cue that drives vergence. However, there is also a dual and parallel feedback loop between vergence and accommodation, and thus one becomes a secondary cue influencing the other [4], [5], [7]. In fact, Suryakumar et al. in [8] measure both vergence and accommodation at the same time during the viewing of stereoscopic imagery, establish that accommodative response driven from disparity and resultant vergence is the same as the monocular response driven by retinal blur. In a recent review of the topic, [6], Bando et al. summarize some of the literature about this feedback mechanism within the human visual cortex.

In traditional stereoscopic HMD designs, the virtual image is focused at a fixed depth away from the eyes, while the depth of the virtual objects, and hence the binocular disparity, varies with the content [9], [10], which results in conflicting information within the vergence-accommodation feedback loops. Fig. 1 demonstrates the basic geometry of this conflict.

• G. Kramida and A. Varshney are with the Department of Computer Science, University of Maryland, College Park, MD, 20740.
E-mail: gkramida, varshney@umiacs.umd.edu
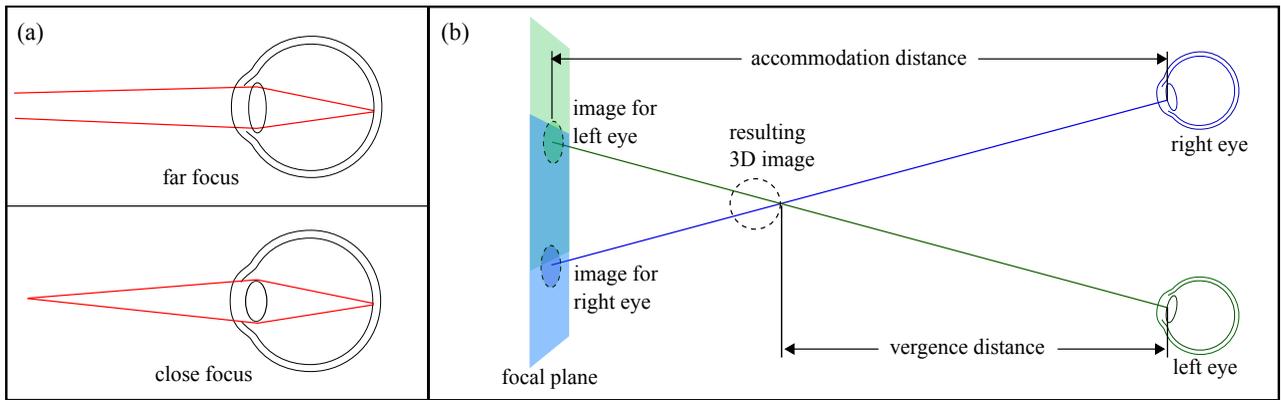
Figure 1. (A) Conceptual representation of accommodation within the same eye. Light rays from far-away objects are spread at a smaller angle, i.e. are closer to parallel, and therefore require little refraction to be focused on the retina. Light rays from close-up objects fan out at a much greater angle, and therefore require more refraction. The lens of the human eye can change in degree of curvature, and, therefore, its refractive index, resulting in a change in focal distance. (B) Conceptual representation of the VAC. Virtual display plane, or focal plane, is located at a fixed distance. The virtual objects can be located either in front or, if it is not at infinity, behind it. Thus the disparity cue drives the eyes to verge at one distance, while the light rays coming from the virtual plane produces retinal blur that drives the eyes to accommodate to another distance, giving rise to the conflict between these depth cues.

The problem is not as acute in certain domains, such as 3D TV or cinema viewing, as it is in HMDs, so long as the content and displays both fit certain constraints. Lambooij et. al in [4] develop a framework of constraints for such applications, the most notable of which in this context being that retinal disparity has to be fall within 1° safety zone with the focal cues. This indeed can be achieved in 3D cinematography, where virtual objects are usually located at a great depth and stereo parameters can be adjusted for each frame prior to viewing. Precise methodologies have been developed on how to tailor the stereo content to achieve this [11], [12], [13], [14].

However, these constraints have to be violated within the context of VR gaming [9], [10], [15] and the context of AR applications [16], where content is dynamic and interactive, and nearby objects have to be shown for a multitude of near-point tasks, for instance – assembly, maintenance, driving, or even simply walking and looking around in a room.

We proceed to outline a hierarchical taxonomy of HMD displays for AR and VR.

## 2 SOLUTIONS

Although the VAC problem remains generally unsolved in modern-day commercial HMDs, researchers have theorized about and built potential prototype solutions since early 1990s. Since the convergence cue in properly-configured stereo displays mostly corresponds[1] to natural world viewing, but the accommodation does not, vast majority of the effort on

resolving VAC gears towards adjusting the retinal blur cue to the virtual depth of the content.

### 2.1 See-through Methods

HMDs for VR are typically opaque, since they only aim to provide an immersive visual of the virtual environment (VE)[2]. For AR, the displays fall into two general categories, optical see-through (OST) and video see-through (VST). Optical see-through systems let through or optically propagate light rays from the real world and use beamsplitters to combine them with virtual imagery. Video see-through displays capture video of the real world and digitally combine it with virtual imagery before re-displaying it to the user. Refer to Table 1 for a comparison of these two methods. Most of the solutions we describe are applicable to both opaque and see-through HMDs, although not all can be as easily integrated into OST as they may be into VST displays.

### 2.2 3D Display Principles

Independently from the see-through method, HMDs can be distinguished based on where they fall on the "extent of presence" axis of the taxonomy for mixed reality displays developed by Milgram and Kishino [19]. HMDs span the range including monoscopic, stereoscopic, and multiscopic displays. We leave out monoscopic heads-up displays from further discussion, since these cannot be used for VR or AR in

---

1. but not entirely, due to offset between virtual camera and pupil, as we discuss later

2. Although it has been suggested to optionally display a minified video-feed of the outside world to prevent the user from running into real obstacles while exploring VEs

|  | Advantages | Drawbacks |
|---|---|---|
| **OST** | provide good peripheral vision and low distortion of the world | difficult to make virtual objects occlude the world |
|  | impose no lag on world imagery | involve complex optical paths: design and fabrication are complex |
|  | imaging point may remain at the pupil | latency between seeing the world and registration for / rendering of virtual content |
|  | no resolution loss for world imagery | mismatch between focal distance of real and virtual objects is more apparent |
| **VST** | easy to make virtual objects occlude world objects in video feed | prone to distort world imagery, esp. in the periphery |
|  | basic designs have fewer optical elements and are cheap and easy to manufacture | impose lag on all content due to video capture, processing, and rendering |
|  | no latency between world imagery and virtual objects | displacement between cameras and pupils contributes to misjudgement of depth and disorientation |
|  |  | resolution and/or FOV loss for world imagery |

Table 1

Comparison of optical see-through (OST) and video see-through (VST) HMDs, based on [1], [17], and [18]

the classical sense (as they cannot facilitate immersive 3D[20]) and are irrelevant to the VAC problem. *Stereoscopic* displays capitalize on rendering a pair of images, one for each eye, with a disparity between the two views to facilitate stereo parallax. *Multiscopic* displays show multiple viewing angles of the 3D scene to each eye. These circumvent VAC in HMDs by rebuilding the entire light field, but introduce other problems.

We base our design classification from these two categories as they tend to address VAC in fundamentally different ways, and further subdivide both branches using the underlying hardware operating principle. Designs from both categories can also be classified based on whether the views are time-multiplexed or space-multiplexed. Please refer to Fig. 2 for the full hierarchical representation of our classification. We proceed to describe the designs in each hardware category in more detail.

### 2.3 Stereoscopic Displays

Each stereoscopic display method can be described as either *multifocal* or *varifocal*, although in certain cases the two techniques can be combined. *Varifocal* designs involve adjustable optics which are able to modify the focal depth of the entire view. *Multifocal* designs, on the other hand, split the view for each eye image into regions based on the depth of the objects within, and display each region on at a separate, fixed focal depth.

Many earlier varifocal display prototypes were built as a proof-of-concept, and could display only simplistic images, often just simple line patterns or wireframe primitives. These either forced the focus information to correspond to the vergence at a single object, or provided some manual input capability to the user to manipulate the X and Y coordinate of the focal point, which in turn would tell the system which object to bring into focus.

Just prior to the turn of the century, *multifocal* designs with physical display stacks were con-
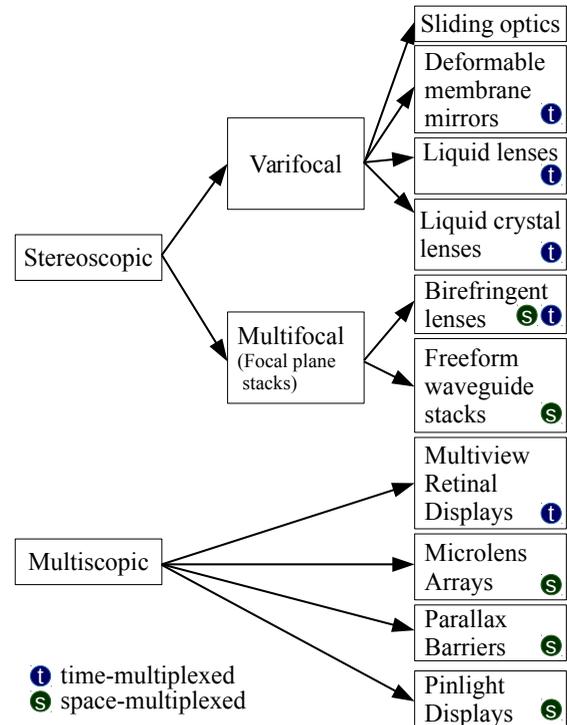


Figure 2. Classification tree of various display designs relevant to HMDs that have shown potential in resolving VAC.

ceived, which to the present day feature solely space-multiplexed focal planes with concurrent output with the exception of [21], which is multiplexed in both space and time. The central idea in those is to display simultaneously on multiple planes at progressively greater focal depths, thus emulating a volume rather than a single image, naturally circumventing VAC. Afterwards, there was an effort to improve and adapt varifocal designs as well to display different images at fixed depth planes in a time-multiplexed fashion.
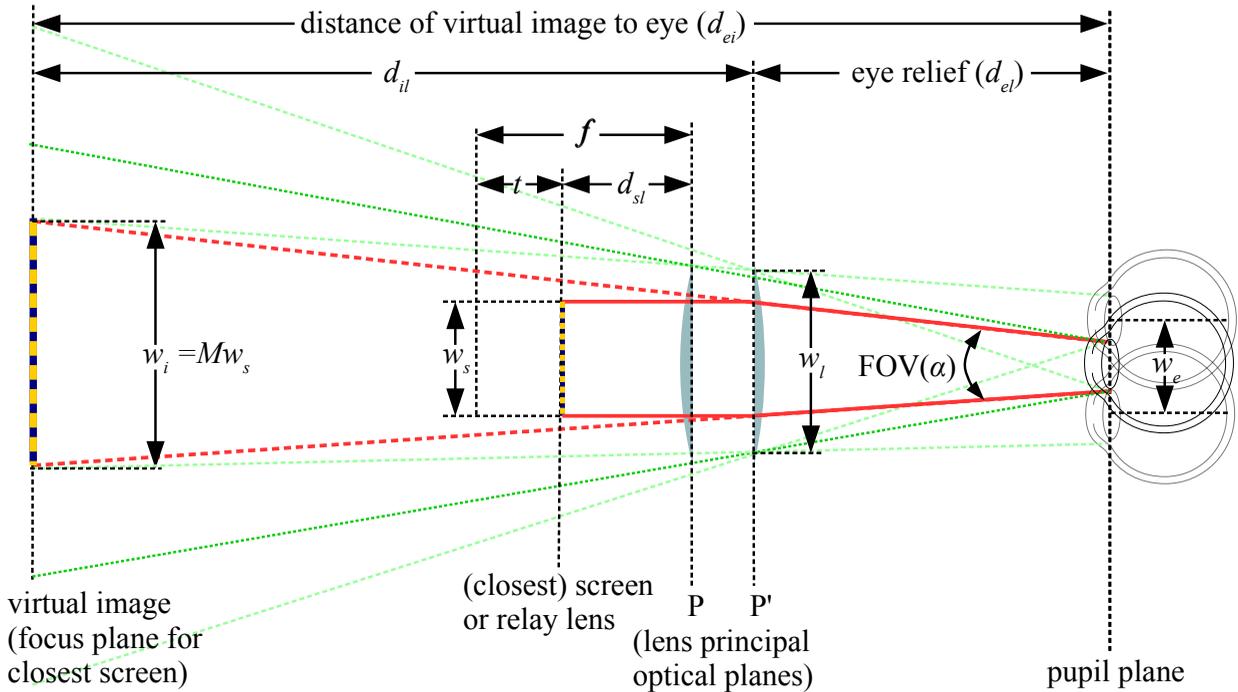
Figure 3. Optics of a simple magnifier. We use this notation for the terms to maintain consistency and to avoid conflicts with other notations. Subscripts $e, i, l,$ and $s$ represent "eye", "(virtual) image", "lens", and "screen" respectively, so terms such as $d_{il}$ explicitly denote "distance from image to lens", and $w_l$ denotes "width of lens." The only exception is $w_e$, which stands for the width of the eye box. $f$ represents focal length of the lens; $t$ represents either the thickness of the display stack (in case of display stack designs) or the range of motion of the relay lens (in case of sliding optics designs); $M$ represents the magnification factor from the screen or relay lens to the virtual image.

Both multifocal and varifocal designs can be described by the optics of a simple magnifier. We establish the notation framework for this in Fig. 3. There exists a common classification which splits optical designs of HMDs into pupil-forming and non-pupil-forming [1], [22], [23]. The simple magnifier embodies all non-pupil-forming designs. The only relevant difference pupil-forming displays have is that they magnify an intermediary image (or a series of such) before relaying, or projecting it, to the final exit pupil. The primary benefit of simple magnifier is that it requires the fewest optical elements, and therefore is relatively light, easy to design, and cheap to manufacture. The primary benefit of the more complex projection systems is that the optical pathway can be wrapped around the head, increasing the optical path length, providing better correction of optical aberrations. For the purposes of this article, it suffices to say that the principles for dealing with VAC as described using the simple magnifier schematics can be applied just as easily to pupil-forming designs by simply replacing the screen with the previous element in the optical path.

### 2.3.1 Sliding Optics

The first experimentally-implemented solution of a varifocal display with mechanically-adjustable focus was that of Shiwa et al. in [24]. In their design, a CRT displayed stereoscopic images for both eyes in two separate sections. Relay lenses were placed in the optical paths between the exit lenses and the corresponding sections of the screen. The relay lenses had the ability to slide back and forth along the optical path, driven by a stepper motor. The authors observe that if the viewer's eyes are located at the focal distance ( $d_{el} = f$ ), when the relay lenses are moved, the angular FOV($\alpha$) remains constant, while the focal distance to the virtual image ($d_{ei}$) changes [3].

The authors suggest that gaze detection should be integrated to determine the exact point, and therefore depth, of the objects being viewed. However, for the purposes of the experiment, their implementation assumed a focal point at the center of the screen and provided manual (mouse/key) controls to move it. Based on the depth of the virtual object at this point, the relay lens for each eye would move along the optical axis, focusing the image at a different distance.

---

3. See Appendix A for mathematical justification

The authors rely on the specifications of the optometer developed in [25][4] to determine that the speed of relay lens movement. They measure that the mechanism takes less than 0.3 seconds to change from 20 cm to 10 m focal plane distance (5 and 0.1 diopters respectively), which they conclude is fast enough to keep up with eye accommodation. A recent study on accommodation responses for various age groups and lighting conditions confirms this to be true [26][5]: the youngest age group in the brightest setting showed an average peak velocity of only $1.878 \pm 0.625$ diopter/sec.

Yanagisawa et al. also construct and analyze a 3D display of similar design with an adjustable relay lens [27]. Both systems have angular FOV below $50°$. Shibata et al. [28], rather then changing the position of a relay lens, change the axial position of the actual display in relation to the exit static mono-focal lens according to the same principle, varying focal depth from 30 cm to 2 m (3.0 to 0.5D).

All of the above-mentioned displays with mechanically-adjustable focus are large and cumbersome bench systems, and thus would require significant effort to be scaled down to be used in portable HMDs. Since the optics for HMDs cannot physically span the entire near range where the VAC conflict is significantly acute, downsizing of such designs would require additional magnification of the virtual image.

### 2.3.2 Deformable Mirrors in Virtual Retinal Displays

First proposed in [29], a virtual retinal display (VRD) projects a low-laser light beam directly into the pupil, forming the image on the back of the retina directly rather than on an external device, which makes it radically different from other display technologies. In [30], McQuaide et al. at the Human Interface Technology Laboratory (HITLab)[6] use a virtual retinal display (VRD) in conjunction with micro-electromechanical system (MEMS) deformable mirrors. The VRD scans the laser light onto the deformable mirror, which reflects it through a series of pivoting mirrors directly into the pupil in an x-y raster pattern. In this way, the VRD directly forms the image on the retina. The MEMS mirror is a thin circular membrane of silicon nitride coated with aluminum and suspended over an electrode. The surface of the mirror changes its convergence depending on how much voltage is applied to the electrode, thus directly modifies the focus of the laser beam, altering the required accommodation to view the displayed objects without blur. The authors achieve a continuous range of focal planes from 33 cm to infinity (3.0 to 0.0 D), which is later improved

to 7cm to infinity in [31]. The experiments feature a monocular table-top proof-of-concept system which projected very basic images (two lines), but showed that observers' accommodative responses coherently matched changes in the focal stimulus demands controlled by the mirror.

While deformable mirrors can be used in a varifocal fashion, focusing on the one depth being observed, they also can be flipped fast enough between two focal planes to create the illusion of contiguous 3D volume. Research on VRDs with deformable membrane mirrors is continued in [32], where Schowengerdt et al. of HITLab synchronize the membrane curvature changes with per-frame swapping between two different images, thus displaying the images at different depth simultaneously and simulating the light field. The prototype's depth range spans contiguously from 6.25 cm to infinity.

The claimed advantage of the VRD designs is that they can potentially be made less bulky, since they do not require an actual image-forming display. However, there still needs to be a reflective surface spanning a large area in front of the observer's eyes in order to project an image with a large angular FOV.

### 2.3.3 Liquid and Electroactive Lens Displays

The very first to use a liquid lens for dynamically switching the perceived focus in a display were Suyama et al. in [33]. The lens could be adjusted to any optical power between -1.2 to +1.5 diopters at a frame rate of 60 Hz. Another static lens was placed between the exit pupil and the varifocal lens, in order to keep FOV of the output image constant. The prototype featured a single 2D display, providing only the movement parallax without the binocular disparity. In the experiment, simple 3D primitives were shown, whose focal depth was controlled.

Years later, Liu and Hua build their own proof-of-concept monocular liquid-lens varifocal prototype in [34]. The liquid lens they used could change from -5 to +20 diopters within 74 ms (7 Hz), but they also test the speed of several alternative lenses, with speeds up to 9 ms (56 Hz), which approach the 60 Hz frequency. The optics of the whole system are set up to vary accommodation from 0 to 8 diopters (infinity to 12.5 cm). They continue their research in [35], where they integrate the 9 ms liquid lens and have it oscillate between two different focal planes, thus emulating a light field at about 37.5 Hz.

One problem with the liquid lens that Liu and Hua identify is that, during settling time of the liquid lens when its driving signal is switched, there are longitudinal shifts of the focal planes, which yield minor image blur and less accurate depth representations. They hypothesize this problem can be mitigated by a liquid lens with a yet faster response time. Subsequently, in [36], Liu et al. integrate their liquid lens mechanism into an HMD. The prototype's

---

4. This optometer detected accommodation to within $\pm 0.25$ diopters (1 D = 1/m) at the rate of 4.7 Hz.
5. The subjects focused from a target at 4m to a target at 70cm away
6. www.hitl.washington.edu

FOV spans only about 16° horizontally. They test it on ten subjects and determine their error rate in a basic depth estimation task, as well as measuring the actual accommodation response with a near-infrared autorefractor, concluding that their approach yields a better accommodation cue than static optics.

A critique of the liquid lenses by Love et. al in [21] is that a switchable-focal-plane display requires a minimum of four states, not two, and, provided a liquid lens frequency of 60 Hz (which lenses used by Liu et. al do not yet achieve but target for future research), the display could yield an maximum refresh rate of only 12.5 Hz, and hence would produce flicker and motion artifacts.

However, there exist other methods to adjust optical power of a lens besides actually changing its geometry, as in the liquid lens. One possible alternative is the liquid crystal electroactive lens, as also suggested by Liu and Hua in both [34] and [36]. Such lenses consist of a layer of liquid crystal sandwiched between two (often planar) glass substrates [37]. The two substrates are coated with (transparent) indium tin oxide on sides parallel to the optical axis, and with aluminum film on the other sides; these two materials act as electrodes. Liquid crystal itself consists of thin rod-like molecules. A fixed voltage is applied to the side aluminum electrodes, the molecules are aligned homogeneously parallel to the substrates. When additional voltage is applied to the indium tin oxide electrodes, the molecules assume a different homogeneous angle closer to perpendicular, which varies with the voltage. Hence, modulating the voltage on the indium oxide changes the refractive index and therefore the optical power.

Ye et al. demonstrate a liquid crystal lens with controllable power between 0.8 and 10.7 D (from about 9 cm to 1.25 m) [37]. Li et al. develop and implement a glasses-thin prototype of adjustable eyewear for use by far-sighted people (presbyopes), whose optical power varies dynamically between +1.0 and +2.0 D [38]. A slew of research was done on prototypes of bench autostereoscopic displays using a liquid crystal lens arrays to control the focal depth of individual pixels or image regions [39], [40], [41], [42], [43], [44], [45], [46], [47]. Yet we are not aware of any work that integrates liquid crystal lenses into HMDs in practice or develops any theoretical framework for this.

### 2.3.4 Focal Plane Stacks

The concept of spatially-multiplexed multifocal designs originates from a study by Rolland et al. [48], who explore the feasibility of stacking multiple display planes, each focused at its own depth, and rendering different images to them simultaneously. The original idea is, at each plane, to leave those pixels that correspond to a different depth layer transparent, while rendering only those objects that correspond. The viewers would then be able to naturally converge

on and accommodate to the correct depth, wherever they look. Authors develop a mathematical model that stipulates at what intervals to place the focal planes (dioptric spacing), as well as requirements for the total number of planes and pixel density of the displays. They determine that a minimum of 14 planes is required to achieve a focal range between 2 diopters and infinity, with interplanar spacing at 1/7 diopters.

They also suggest that if a fixed positive lens is positioned in front of the focal planes, physical thickness of the display can be greatly reduced. Their framework is analogous to fig. 3, so the thickness of the resulting display stack can be expressed as:

$$t = f - d_{sl} = \frac{f^2}{f + d_{il}} = \frac{f^2}{f + d_{ei} - d_{el}} \qquad (1)$$

In the above equation, $d_{ei}$ is the shortest depth the viewer should be able to accommodate to, while $d_{sl}$ is the offset from the lens to first screen in the stack, which displays virtual objects at that depth. $d_{sl}$ can be expressed as:

$$d_{sl} = \frac{1}{\frac{1}{f} + \frac{1}{d_{il}}} = \frac{f d_{il}}{f + d_{il}} \qquad (2)$$

Based on these equations[7], for a 30 mm focal length, 25 cm closest viewing distance, and 25 mm eye relief, $d_{sl}$ would be approx. 26.5 mm and the stack thickness $t$ would be approx. 3.5 mm, resulting in an overall minimum display thickness of about 3 cm. Authors proceed to derive the resolution requirements for such displays and conclude they can be built using contemporary technology.

However, as [36] points out, a practical application of this method is still challenging, since no display material known to date has enough transmittance to allow light to pass through such a thick stack of screens. Akeley et al. are the first to address this challenge in [49]. They design and build a prototype with only three focal planes per eye, all projected to via beamsplitters and mirrors from 6 viewports rendered on a single high-resolution LCD monitor. Their main contribution is a depth filtering algorithm, which they use to vary pixel intensity linearly with the difference between their virtual depth and the depth of the actual plane on which they are shown, thus emulating the light field in between the viewing planes. Although this prototype shows that sparse display stacks can be effectively used, it is still a large, immobile table-top machine, and needs to be scaled down to be used as an HMD.

After developing the liquid lens HMD, Liu and Hua switch gears and also come up with an elaborate theoretical framework for using specifically *sparse* display stacks in HMDs in [50], coining term depth-fused 3D displays (DFD) for any display with depth

---

7. See appendix B for detailed derivations of these equations, which not given in the original source

blending. There are two major points their framework addresses: (1) the dioptric spacing between adjacent focal planes, now different from Akeley's model in that it is based on depth-of-field rather than stereoacuity, and (2) the depth-weighted blending function to render a continuous volume (also referred to as depth filtering). They develop their own depth blending model, different from the one described by Akeley in [49].

In a later work, Ravikumar et al. analyze both of these blending models, and find that Akeley's linear model is theoretically better based on contrast and effectiveness in correctly driving accommodation cues [51]. MacKenzie et al. [52] *experimentally* establish requirements for plane separation in display stacks with depth blending: a 8/9 D separation, yielding a minimum of five planes for a depth range from 28 cm to infinity (32/9 to 0 D). They also note that contrast (and, therefore, sharpness) is attenuated due to one or more planes between the eye and the target being defocused, an effect present even at 8/9 D and more drastic at larger plane separations. This is an inherent flaw in all multifocal systems, which causes rendered objects to always appear different from and less sharp than naturally-observed objects.

### 2.3.5  Birefringent Lenses

Love et al. in [21] build a similar display to that of Akeley et al., but their design is time-multiplexed using light polarization. They used two birefringent lenses out of calcite interspersed with polarization switches. They take advantage of the fact that, while calcite is highly transparent, birefringent lenses have two different indices of refraction, one for light polarized along one crystalline axis and another for the light polarized along the orthogonal axis. Thus, for light with different polarization, the lenses would have different optical power, and focus to planes at different distances. This way, the setup features only two lenses, but projects to four different depths. They use the shutter technique for switching between volumetric slices of images with different polarization, and achieve a frame-rate of 45 Hz using two CRT monitors, one for each eye. The design demonstrates superior transmittance between focal planes. However, the prototype is still not small enough to be used as an HMD.

### 2.3.6  Freeform Waveguides

Our eyes do not come retrofitted within threaded circular nests. If that were the case, designing a lightweight, super-compact, wide-FOV HMD with conic optics would be trivial. Hence, although stacked display designs with conic optics can be said to have "evolved" into freeform optics displays, as Rolland and Thompson semi-humorously note in [53], the advent of automatic fabrication of surfaces under computer numerical control (CNC) in the past two

decades constitutes a revolution in HMD designs and other optics applications. Indeed, freeform optics provide HMD researchers with a much greater freedom and flexibility than they had with conventional rotationally-symmetric surfaces. We first provide some historical context about freeform optics in HMDs as the precursor of resulting VAC solutions.

We suppose that the time and place at which freeform optics started to heavily affect HMD designs, especially optical see-through HMDs, would be just after the beginning of this century, at the Optical Diagnostics and Applications Laboratory (the O.D.A. Lab) of Rochester University, headed by the mentioned Rolland. In [54], Cakmakci et. al target eyeglasses form factor and see-through operational principle as the primary display in wearable computing in the future. They put forth a set of optical and ergonomic requirements for such a display. They also propose a prototype, minimizing the number of optical elements. They capitalize on the original idea in a patent by Bettinger [55] by placing the actual microdisplay off the optical axis. To achieve this, they still propose a radially symmetrical lens, but in conjunction with a freeform mirror to guide the light to the exit pupil. They publish the particulars of the fabrication process in [56]. The prototype has a monocular 27° x 10° FOV, 640 x 480 pixel display, and a fixed focal length of 32mm. The Cakmakci et al. evaluate their design in [57] and [58] and discuss how Gaussian Radial Basis Functions (RBFs) yield an advantage over Zernike polynomials and anamorphic spheres when used to optimize surfaces for freeform optics with potentially non-circular apertures. In [59], Kaya et al. describe a method for determining the number of basis in RBFs required to achieve desired accuracy for optics applications.

Cheng et al. building on earlier work at the O.D.A. lab, propose to use tiled freeform prisms for a binocular optical see-through HMD prototype to achieve a much wider FOV, 56° x 45° per eye, or, potentially, a 119° x 56° total binocular resolution [60]. We note that Hua, presently of University of Arizona, who earlier collaborated with Liu on [34], [36], and [50], was one of the authors. Two years later in [61], most of the same researchers publish the particulars of the fabrication process and evaluation of the resulting prototype. In parallel, Chunyu et al. under direction of Dr. Hua, modify the design such that, theoretically, it can display opaque virtual imagery even in outdoor environments. Meanwhile, Cheng et al. advance the design to actually stack the freeform prisms, thereby proposing a spatially-multiplexed multifocal display and addressing the VAC [62].

One critique of using the tiled freeform prism approach is that it is still much bulkier than ordinary eyeglasses [63]. For instance, the design in [60] could not be made thinner than 1.7 cm. Part of the problem is that, if freeform prisms are used guide the digital

imagery, additional prisms are required in order to undistort the light coming in from the environment. Another problem is that depth-blended multifocal designs with freeform waveguides are still prone to the contrast and sharpness loss problem described by MacKenzie et al. in [52].

Also, the multifocal design by Cheng et al. only features two focal planes, separated by 0.6 D, yielding a range from 1.25 to 5m. While separation adheres to the prescribed formula, not being able to accommodate within 1.25 meters possibly inhibits any tasks involving hand manipulation, although the amount of visual discomfort resulting from this more limited decoupling of vergence and accommodation has yet to be empirically measured. Adding more focal planes would also increase the number of needed lenses and the thickness of the display, while spreading the focal planes farther apart will impose critical contrast loss.

## 2.4 Multiscopic Displays

Recently, *multiscopic displays* (also referred to as *computational displays*, and *light field displays*) have emerged as a prominent research direction within the HMD context. The underlying principle these displays use is called integral imaging, which involves generating multiple light rays from *the same* point in the scene such that they intersect within the eye at different *perceived* depths, thereby emulating a contiguous *light field* within the eye. The only time-multiplexed multiscopic HMD design known to date relies on high-update-frequency display elements and a galvanometer to generate the needed rays. In contrast, the spatially-multiplexed multiscopic designs achieve this using fine arrays (or layers of arrays) of microscopic optical elements, such as spatial light modulators, microlenses, and/or point light sources ("*pinlights*").

### 2.4.1 Multiview Retinal Displays

In [64], Kim et al. build and analyze an HMD prototype that uses a rotating galvanometer scanner synchronized to a digital micromirror display[8] panel alternating between 26 slightly-different viewpoints of the scene. They use a galvanometer to change the angle at which rays from the display fall on a relay lens for each viewpoint, which then propagates the rays through the observer's pupil onto the retina.

The resulting views are called *elemental images* [65]. Displays using this technique are often referred to as *multiview displays* [66]. We discuss this technique in greater detail below. Kim et al. analyze the light field produced by their system by placing a camera at eye's location and recording a 3D sequence of moving lines shown by their display, and conclude that focal cues produced are good enough to control the eye's accommodative response.

### 2.4.2 Microlens Arrays

Lanman and Luebke at Nvidia Research come up with their own computational display prototype using a microlens array to magnify the image produced by an OLED screen [67]. They subdivide the screen into multiple tiles, each showing the same 3D scene, but projected slightly off-axis in all but the central view. Due to the need for overlap between views, this greatly reduces the spatial resolution of the display[9]. Instead of a single magnifier lens, they use a sheet of microscopic lenses, such that each lens magnifies its own tile, thereby forming a *super-multiview* display.

Fig. 4 shows the principle operating behind this display. Rays from the same point in the virtual scene are relayed by multiple lenses into different locations on the pupil. The spread of these rays on the pupil varies with the offset of the point from one display section to the other. Rays from closer objects have a wider spread, while rays from more distant objects are closer to parallel, mimicking the natural viewing situation. Due to the small size of each lens, the circle of confusion for a ray bundle coming from each lens, denoted by $c$, is smaller than the eye resolution, so long as the virtual objects stay within range requirements. At the same time, the circle of confusion $c'$, generated by ray bundles from multiple lenses, emulates retinal blur. Hence, the eye tends to accommodate to objects within the virtual scene rather than the virtual image plane, but at a great expense to spatial resolution, which, the authors believe, may soon become acceptable given current technology trends. However, increasing resolution of the display also means increasing microlens density, which, in turn, causes increased diffraction and unwanted blur.

Another drawback of this design is that it may only support the video-see-through operational model, since microlenses would distort natural light and the display would effectively block it. Song et. al address this in [68], proposing an optical see-through design using either microlenses or pinholes together with pair of freeform prisms. The first prism guides light rays from the optical micro-structures, which are located off to the side, while the second prism compensates for distortion of light rays from the environment. This design, however, suffers from the same excessive thickness problem as [60] and [62].

### 2.4.3 Parallax Barriers

Parallax-barrier multiscopic displays have recently been adapted for usage in HMDs by Maimone et al. in [63]. They use multiple layers of spatial light modulators placed between the display and the eye. The stack acts as a *parallax barrier*, where light rays are modulated spatially and angularly as they pass

---

8. Digital micromirrors are a type of spatial light modulators used in digital light processing (DLP). Their main advantage is really high update frequency.

9. The physical 1280x720 pixel OLED display of the prototype yielded an effective spatial resolution of 146x78
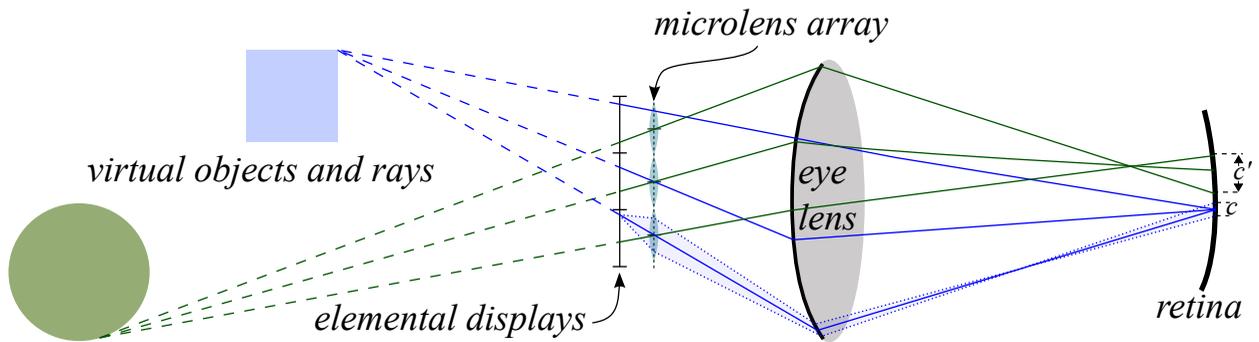
Figure 4. Conceptual diagram of a microlens head-mounted display. Eye is focused on the corner of the virtual blue box, while the green sphere appears out-of-focus.

through and reach the eye. The sums of perceived light ray intensities are synthesized at precise locations on the pupil, such that the eye accommodates naturally to the depth of the displayed virtual object and its representation comes into focus on the retina.

Due to resolution, display update frequency, and layer density limitations, each ray in the light field cannot physically be synthesized accurately. Rather than trying to replicate the exact original light field, Maimone et al. come up with what they call *retinal optimization*. They constrain groups of rays falling at the same spot on the pupil by the perceived sum of their intensities. They note that exact retinal optimization would require knowledge of the eye lens' focus in order to determine where rays will fall on the retina. Instead of determining the state of the lens, they perform the optimization as if the eye is simultaneously focused on each object in the scene, at expense to retinal blur quality.

Another setback is that ray generation for each layer at each time step is performed using compressive optimization, a process in which random noise, different at each layer, is inherent in the output. The simple solution is to let noise produced at each modulator layer to cancel out in the final image. This works to a degree, but the resulting image still comes out slightly blurred, in part due to diffraction of the light as it comes through the barrier. Another problem is that of pure computational efficiency: the optimization performance Maimone et al. use, specifically, content-adaptive parallax barriers [69], takes a few minutes for a single image. However, they note that faster methods have been proposed, such as the adaptive sampling framework developed by Heide et. al in [70], which uses only 3.82% of the rays in the full target light field.

The prototype display assumes there is no relative motion between the pupil and the display. In a natural setting where the gaze direction is unconstrained, in order to synthesize the light-field correctly at each instance, eye tracking would have to be integrated into the HMD. We discuss advances in this aspect

in the following section. The performance of their design was also constrained by the LCD panel refresh rate and pixel density. The authors believe these limitations will be alleviated by upcoming display technology.

Maimone et. al test their prototype display by substituting the eye with a camera and conclude that the design has both promising occlusion quality and the generated image appears mostly in focus when focal distance of the camera corresponds to the depth for which the image was optimized.

### 2.4.4 Pinlight Displays

Maimone and Lanman combine their efforts in [71] to tackle these problems. They design and fabricate a *pinlight* head-mounted display, which also uses a form of integral imaging, but instead of microlenses uses a dense array of point light sources, projected through a barrier of liquid crystal modulator arrays[10], onto the eye. The light sources are simply cavities etched into a sheet of transparent plastic, which light up when much coarser diodes shine light into the plastic from the perimeter. The LCD forms elemental images, one for each point light source, onto the eye, thus approximating the light field. This design allows, to some degree, to control both the amount of light from the point light sources and the amount of natural light from the environment that reach the eye.

Aside from optical-see-through capabilities, an advantage of this pinlight display is its compactness, which easily allows for a wide field of view. The prototype features a 110° FOV, never achieved before in any optical-see-through head-mounted display, with an eye-glasses form factor. Diffraction remains a major problem in all of these displays, placing a hard limit on the resolution achievable without alluding to eye tracking for fovea-contingent display schemes.

## 2.5 Eye Tracking in HMDs

The previously-described stereoscopic designs project to multiple depths (in a time- or space-multiplexed

10. essentially, an LCD panel

fashion), emulating the light field in a discrete fashion, in contrast to the multiscopic displays, which emulate it in a contiguous fashion. As an alternative, it has been theorized that the adjustable optics in the varifocal methods can also be gaze-driven[36],[72], adjusting focus specifically to the depth of the virtual point where the viewer looks at any given moment. Authors of several works we discuss hypothesized about integrating an eye tracker into an HMD to accomplish this. In fact, some work has been done specifically on designing eye-tracked HMDs (ET-HMDs [73]) in a compact, ergonomic way, which can potentially be used for this and other purposes. As mentioned earlier, multiscopic displays could also benefit from eye-tracking to circumvent necessity of excessive microstructure density, which causes aberrations due to diffraction [67].

So far, several studies have used eye-trackers in conjunction with emulated (software-rendered) retinal blur, investigating the effects on accommodation. Alternative stereo vergence models driven by eye-tracking have also been explored. However, to our knowledge, no eye-tracker-driven varifocal design has yet been published.

In this subsection, we first cover work that has been done to integrate Eye Tracking into HMDs, and proceed to describe how eye tracking has been applied to mitigate the VAC conflict.

### 2.5.1 Integration of Eye Tracking in HMDs

There have been early instances of integrating eye tracking hardware into off-the-shelf VR headsets. One such effort by Beach et. al proposed to track gaze to provide a hands-free interface[74] to the user. In parallel, Duchovski integrates an existing eye tracker with a bench display, stipulating it may allow for *foveated rendering*, or outputting greater detail exactly at the users gaze point in a "just in time" fashion. Later, Duchowski et al. integrate the ISCAN tracker into an off-the-shelf VR HMD to train and evaluate visual inspection of aircraft cargo bays [75]. Hayhoe et al. use the same headset integrated with an off-the-shelf magnetic tracker for the head and another near-infrared (NIR) eye tracker in order to study saccadic eye movements on subjects performing simple tasks in virtual environments.

Vaissie and Rolland make the first efforts in designing a fully-integrated eye-tracked HMD (ET-HMD) [76], [77]. They propose that ET-HMDs can be used to place the virtual cameras rendering virtual objects at virtual locations that correspond to pupil locations rather than eyeball centers of the user [78], eliminating a convergence disparity that still plagues commercial HMD designs today.

In [79], Hua develops a prototype of a fully-integrated optical see-through ET-HMD using an infrared tracker and an ISCAN circuit board. In [80] adapts the design to head-mounted projectiv displays

(HMPD). In [81], Hua et. al develop corneal reflection eye-tracking methods and algorithms for ET-HMDs which are more tolerant to slippage than the alternatives. In [82], they devise the proper eye illumination model for such tracking. David et al. in [83] design and simulate their own ET-HMD, with the novel feature comprising the integration of the NIR sensor with the LCoS[11] microdisplay on a single CMOS chip.

In [73] and [72], Hua et al. design and build a new optical see-through ET-HMD prototype with the glint tracking and illumination model in mind, but also using freeform waveguide to direct both the optical path of the display and the eye imaging, making the overal desgin much more compact. It features an 80° by 50° elliptical FOV[12], with some distortion beyond the central 50° area. They further refine their design in [84].

### 2.5.2 Manipulating Depth Cues using Eye Tracking

Mantiuk et al. were the first to implement gaze-dependent *rendered* depth-of-field (DOF) using eye tracking. They use a commercially-available glint-based eye tracker on a standard 22" LCD without stereo. Their algorithm determined focal blur by relative distance between the object gazed upon and other objects around it. Their experiment with 20 live subjects viewing animated and static virtual environments confirmed that the DOF effect guided by eye movements is preferential to predefined DOF effect. Vinnikov and Allison follow suit and test a similar system with stereoscopic bench display on a group of users viewing 3D scenes, and, based on the results of a questionnaire, conclude that simulated focal blur guided by eye tracking subjectively enhances the depth effect when combined with stereo [85]. Finally, Duchowski et. al. conduct another gaze-contingent focal blur study with a stereo display and binocular eye-tracker. The depth blur amount in their system is deduced directly from vergence, i.e. from triangulating the intersection of the gaze vectors for each eye. Their user study concludes that gaze-driven simulated DOF significantly reduces visual discomfort for people with high stereo-acuity.

Although these studies suggest that gaze-driven rendered blur contributes to visual comfort, this kind of blur alone has been both theoretically and experimentally shown not to drive accommodation: the light rays coming from a display focused at at a given depth still diverge at the same angle before reaching the eye lens [85], [86], [87]. These solutions have never been tested in HMDs, but may guide future research on dynamically adjusting optics for varifocal designs.

An approach to addressing VAC radically different from ones aforementioned is that of adjusting vergence to the focal plane instead of the other way

---

11. Liquid Crystal on Silicon
12. compare to 21.4° X 16.1° in Hua Hong's earlier work

around, called dynamic stereoscopy (DS) or dynamic convergence. A pioneering work by State et. al [88] applies dynamic convergence to an augmented reality HMD prototype targeting medical applications. The prototype uses static video cameras, but dynamically adjusts frame cropping to verge on the depth of the central object. Authors discover that DS does in fact mitigate VAC, but introduces another problem, which they refer to as disparity-vergence conflict, which we discuss below. Various DS models have been proposed which rely on salience algorithms to determine the gaze point [9], [10], [15], [89]. Fisker et al. in [90] is the first to use eye tracking integrated into an off-the-shelf VR HMD to do this. They actually report increased eyestrain with their disparity adjustments on, and proceed to improve their system to filter and smooth the adjustments. Later in [91], Bernhard et al. experiment with eye tracking and an autostereoscopic display with a similar DS model, and actually measure fusion time of the imagery as compared to static stereoscopy. They report improvement in fusion times with DS only for virtual objects placed in front of the focal plane, but no significant improvements at or beyond it.

The major problem with DS is what State et al. referred to as the disparity-vergence conflict: adjusting the vergence to the focal plane means that, even though vergence no longer conflicts with accommodation, both cues now indicate the depth of the focal plane rather than the depth of the virtual object. In optical see-through HMDs, this model may suffer problems due to the obvious mismatch between vergence with real-world objects and virtual objects. In video see-through displays, where the disparity of the incoming video stream may also be adjusted (mechanically or via software), further studies are required to determine whether DS will result in misjudging depth to real and virtual objects, although Sherstyuk's preliminary experiment without eye-tracking suggests DS may improve performance in certain VR tasks on nearby objects [89].

## 3 EVALUATION METHODS

We establish four general evaluation strategies to evaluate VAC solutions: (1) subjective user studies, (2) direct measurement of occulomotor responses (3) measurements of physiological fatigue indicators and (4) assessment of brain activity via such tools as EEG or fMRI. Each has its own merits and drawbacks; hence, a combination of several strategies is more robust than a single strategy alone.

### 3.1 Subjective User Studies

User studies are widely accepted and popular as a means to perceptually evaluate stereoscopic viewing experience [4]. These can be subdivided into two main types: performance-oriented, where a user's performance in a task using the evaluated system serves as a measure of effectiveness of the display, and appreciation-oriented, where the user is asked of his/her subjective opinion of their viewing experience. Methodology for appreciation-based surveys of stereoscopic content has been developed in [92]. For general survey methodology, we refer the reader to [93].

Although questionnaires are technologically less involved than any of the other evaluation methods, they are prone to all common pitfalls of subjective measures, such as user bias, problems with quantification, limited population samples which exclude marginal cases, and so on.

### 3.2 Occulomotor Response Measurements

Infrared autorefractors provide an objective and precise measurement of the accommodation response. Despite accurate autorefractors now being widely available in hand-held factors [94], they are still both bulky and expensive, which sets a hurdle for their use with HMDs. An infrared autorefractor determines the eye lens optical power by measuring time-of-flight of infrared light it sends through the pupil, reflected of the inside surfaces, and returning back to its sensors, and thus is a complex mechanism with two optical paths (sending the beam and receiving it) separated by a beamsplitter [95].

Takaki in [96], Shibata et. al in [28], and McQuaide in [30], use autorefractors to measure accommodation responses to their bench prototypes, while Liu et. al in [36] are the only ones yet (to our knowledge) to test an HMD prototype with an autorefractor. Day et al. use an autorefractor to experimentally evaluate effects of depth of field on accommodation and vergence in [86], while MacKenzie et al. in [52] use one to accurately measure accommodation responses of to an adjustable depth-blended focal plane stack display similar that of Akeley et al in [49] in various configurations, in order to establish the focal plane number and separation requirements for multifocal displays.

To measure vergence, one can use a binocular eye tracker as Bernard et al. do in [91]. In [97], Suryakumar et al. build a system with a custom photorefractor and a binocular eye tracker to measure vergence and accommodation to stereo imagery at the same time, which they later apply in [8]. Various ways of integrating eye trackers with or into HMDs have already been discussed, but the integration of a custom photorefractor into an HMD is a complex task, and, to our knowledge, has not yet been attempted. We believe it has potential to provide measurements not only for evaluation, but also for driving varifocal designs.

### 3.3 Fatigue Measurements

The drawback of directly measuring occulomotor response alone is that it does not assess the level of

visual fatigue (asthenopia). While may provide indications of how close the responses are to natural viewing, there are other neurological and psychological factors which may cause different individuals eliciting the same occulomotor responses to experience different levels of discomfort. Studies suggest measuring blinking rate [98], heart rate and heart variability [99], [100], and blood pressure [99], may serve as an objective measure of fatigue during stereo viewing. In addition, standard visual reflex timing measurements can be taken prior to and after the experiment [101].

### 3.4 Brain Activity Measurements

There are yet few studies that measure brain activity to measure fatigue caused by stereo viewing, and virtually none that evaluate VAC-alleviating HMD designs. Hagura and Nakajima perform a preliminary study using fMRI[13] in combination with MEG[14] in order to detect fatigue caused by viewing random-dot stereograms [102]. More recently, Frey et al. perform a pilot study that sheds some light on how visual fatigue due to VAC may be measured using EEG[15] [103].

## 4 DISCUSSION AND CONCLUSION

Head-mounted displays still have a far way to go before they are comfortable enough to be worn by any individual over extended periods of time. VAC remains a major factor contributing to the discomfort, especially for near tasks with VR or AR. We have presented a systematic review of different potential solutions, and now identify gaps in this body of research.

For eyeglasses-form-factor see-through HMDs, the two solutions that appear to have the highest potential are: (1) the under-explored eye-tracked varifocal optics with liquid crystal lenses and (2) eye-tracked computational displays. It also remains to be explored whether birefringent multifocal stereo displays can be minimized to HMD form-factor, although time-multiplexing imposes additional taxing requirements on the display update speed, which is already so critical in HMDs even without it.

Waveguide stacks with more than two focal planes are another under-explored area. Requirements for focal plane stacks have been evaluated based on the criteria of how closely the accommodation response resembles actual live viewing [52], but fatigue levels haven't been measured for designs that don't adhere to the criteria.

For opaque displays, where form factor is not that much of an issue, display stacks and retinal scanning displays definitively represent potential solutions. Retinal scanning displays with deformable

13. Functional magnetic resonance imaging
14. Magnetoencephalography
15. Electroencephalography

mirrors also have the potential to be integrated with eye-trackers in order to dynamically adjust the focal plane.

We anticipate that combinations of various recent advancements, such as freeform waveguides, microlens arrays, DLP mirrors, pinlight display technology, eye tracking, liquid crystal lenses, fiber-scanning displays, and super-high-resolution LCoS displays, will yield much lighter, more ergonomic designs with greater resolution in the near future, and will also greatly alleviate, if not eliminate, side-effects of the VAC.

## APPENDIX A
## MATHEMATICAL DERIVATIONS OF SLIDING RELAY LENS EQUATIONS

This appendix shows how the sliding relay lens is able to change the focal depth while maintaining a constant FOV. Please refer to Fig. 3 for a schematic with variables.

We begin with the Gaussian Lens formula derived in section 5.2.3 of [104] from the *thin lens equation*, itself derived directly from Snell's Law of refraction.

$$\frac{1}{f} = \frac{1}{d_{sl}} - \frac{1}{d_{il}} \tag{3}$$

Simple magnification retains the proportion of the throw distance to the size of the object along the focal plane, hence the magnification factor can be expressed as:

$$M = \frac{w_i}{w_s} = \frac{d_{il}}{d_{sl}} \tag{4}$$

By rewriting eq. 3 as

$$d_{sl} = \frac{f d_{il}}{f + d_{il}} \tag{5}$$

and substituting it into 4, we arrive at:

$$M = \frac{w_i}{w_s} = 1 + \frac{d_{il}}{f} \tag{6}$$

Recall that the specified condition is that eye relief must equal the focal depth, i.e. $d_{el} = f$.

This leads to:

$$M = 1 + \frac{d_{ei} - d_{el}}{f} = 1 + \frac{d_{ei} - f}{f} = \frac{d_{ei}}{f} \tag{7}$$

In this case, angular FOV is limited by $w_i = M w_s$, and can be expressed as:

$$\alpha = 2 \arctan\left(\frac{M w_s}{2 d_{ei}}\right) \tag{8}$$

Figure 5. Basic layout of a magnifier as adapted from Rolland et. al in [48]. $Lm$ corresponds to $d_{ei}$ in our nomenclature, $X_{Lm}$ is $d_{sl}$, $ER$ is $d_{el}$, and $dx$, the stack thickness, is $t$. Note that the x axis is inverted relative to direction of these vectors.

We substitute eq. 7 into eq. 8 to obtain:

$$\alpha = 2\arctan\left(\frac{d_{ei}w_s}{2fd_{ei}}\right) = 2\arctan\left(\frac{w_s}{2f}\right) \qquad (9)$$

Thus, $\alpha$ only depends on the width of the relay lens and the focal distance, which are constant. On the other hand, by rewrighting eq. 3 we obtain:

$$d_{il} = \frac{fd_{sl}}{f - d_{sl}}, \qquad (10)$$

which shows that the focal distance $d_{ei}$ varies with the distance to the relay lens, reaching infinity at $d_{sl} = f$.

## APPENDIX B
## MATHEMATICAL DERIVATIONS OF DISPLAY STACK PARAMETER EQUATIONS

This appendix shows the step-by-step mathematical derivations of the equations for display stack from [16] and [48]. Please refer to Fig. 5 to match variable names when consulting the original source.

The first is the imaging equation,

$$\frac{1}{x'} = \frac{1}{x} - \frac{1}{f}, \qquad (11)$$

where $x$ and $x'$ are distances of a single display pane from principal plane P and of the image to principal plane P', respectively. $x'$ falls within the range $[d_{ei}, infty]$, while $x$ varies within $[d_{sl}, f]$, with $t$ representing the total span of the latter interval (see Fig. 3).

We plug in the left (closest) limits for $x'$ and $x$:

$$\frac{1}{d_{ei}} = \frac{1}{d_{sl}} - \frac{1}{f}, \qquad (12)$$

We solve for $x_{sl}$, which in this case represents the stack distance from the lens:

$$d_{sl} = \frac{f(d_{il})}{f + d_{il}} \qquad (13)$$

In [49], the following equation for the depth of the display stack is given:

$$d = \frac{1}{(n^* + (1/14))} \quad (m), \qquad (14)$$

where $n^*$ is the optical power of the lens and $1/14$ is the optical power of the most distant plane. In order to tie equations 13 and 14, it is necessary to express $n^*$ as $1/f$ and replace $1/14$ with $1/(Lm - ER)$ (since the value of ER is very small in comparison with $Lm$, i.e. about 0.25 m, Akeley et. al omit it). We thus obtain:

$$d_{sl} = \frac{1}{\frac{1}{f} + \frac{1}{d_{ei} - d_{el}}}, \qquad (15)$$

which can be easily rewritten as equation 13. Finally, from 13, we obtain the equation for the stack depth:

$$\begin{aligned} t &= f - x_{Lm} \\ &= f - \frac{fd_{il}}{f + d_{il}} \\ &= \frac{f^2 + fd_{il}}{f + d_{il}} - \frac{fd_{il}}{f + d_{il}} \\ &= \frac{f^2}{f + d_{il}} \end{aligned} \qquad (16)$$

## REFERENCES

[1] O. Cakmakci and J. Rolland, "Head-worn displays: a review," Display Technology, Journal of, vol. 2, no. 3, pp. 199–216, 2006. [Online]. Available: http://ieeexplore.ieee.org/xpls/abs_all.jsp?arnumber=1677544

[2] S. R. Bharadwaj and T. R. Candy, "Accommodative and vergence responses to conflicting blur and disparity stimuli during development." Journal of vision, vol. 9, no. 11, pp. 4.1–18, Jan. 2009. [Online]. Available: http://www.journalofvision.org/content/9/11/4.short

[3] D. M. Hoffman, A. R. Girshick, K. Akeley, and M. S. Banks, "Vergence-accommodation conflicts hinder visual performance and cause visual fatigue." Journal of vision, vol. 8, no. 3, pp. 33.1–30, Jan. 2008. [Online]. Available: http://www.journalofvision.org/content/8/3/33.short

[4] M. Lambooij, W. IJsselsteijn, M. Fortuin, and I. Heynderickx, "Visual Discomfort and Visual Fatigue of Stereoscopic Displays: A Review," Journal of Imaging Science and Technology, vol. 53, no. 3, p. 030201, 2009. [Online]. Available: http://umd.library.ingentaconnect.com/content/ist/jist/2009/00000053/00000003/art00001

[5] S. Reichelt, R. Häussler, G. Fütterer, and N. Leister, "Depth cues in human visual perception and their realization in 3D displays," in SPIE Defense, Security, and Sensing, B. Javidi, J.-Y. Son, J. T. Thomas, and D. D. Desjardins, Eds. International Society for Optics and Photonics, Apr. 2010, pp. 76 900B–76 900B–12. [Online]. Available: http://proceedings.spiedigitallibrary.org/proceeding.aspx?articleid=1344889

[6] T. Bando, A. Iijima, and S. Yano, "Visual fatigue caused by stereoscopic images and the search for the requirement to prevent them: A review," Displays, vol. 33, no. 2, pp. 76–83, Apr. 2012. [Online]. Available: http://www.sciencedirect.com/science/article/pii/S0141938211000825

[7] G. K. Hung, K. J. Ciuffreda, and M. Rosenfield, "Proximal contribution to a linear static model of accommodation and vergence." Ophthalmic & physiological optics : the journal of the British College of Ophthalmic Opticians (Optometrists), vol. 16, no. 1, pp. 31–41, Jan. 1996. [Online]. Available: http://www.ncbi.nlm.nih.gov/pubmed/8729564

[8] R. Suryakumar, J. P. Meyers, E. L. Irving, and W. R. Bobier, "Vergence accommodation and monocular closed loop blur accommodation have similar dynamic characteristics." Vision research, vol. 47, no. 3, pp. 327–37, Feb. 2007. [Online]. Available: http://www.sciencedirect.com/science/article/pii/S0042698906004937

[9] A. Sherstyuk and A. State, "Dynamic eye convergence for head-mounted displays," Proceedings of the 17th ACM Symposium on Virtual Reality Software and Technology - VRST '10, p. 43, 2010. [Online]. Available: http://portal.acm.org/citation.cfm?doid=1889863.1889869

[10] T. Oskam, A. Hornung, H. Bowles, K. Mitchell, and M. Gross, "OSCAM - optimized stereoscopic camera control for interactive 3D," p. 1, 2011.

[11] A. Shamir and O. Sorkine, "Visual media retargeting," in ACM SIGGRAPH ASIA 2009 Courses. ACM, 2009, p. 11.

[12] M. Lang, A. Hornung, O. Wang, S. Poulakos, A. Smolic, and M. Gross, "Nonlinear disparity mapping for stereoscopic 3d," ACM Transactions on Graphics (TOG), vol. 29, no. 4, p. 75, 2010.

[13] C.-W. Liu, T.-H. Huang, M.-H. Chang, K.-Y. Lee, C.-K. Liang, and Y.-Y. Chuang, "3d cinematography principles and their applications to stereoscopic media processing," in Proceedings of the 19th ACM international conference on Multimedia. ACM, 2011, pp. 253–262.

[14] P. Didyk, T. Ritschel, E. Eisemann, K. Myszkowski, H.-P. Seidel, and W. Matusik, "A luminance-contrast-aware disparity model and applications," ACM Transactions on Graphics (TOG), vol. 31, no. 6, p. 184, 2012.

[15] U. Celikcan, G. Cimen, E. B. Kevinc, and T. Capin, "Attention-aware disparity control in interactive environments," in User Modeling and User-Adapted Interaction, vol. 29, no. 6-8, 2013, pp. 685–694. [Online]. Available: http://link.springer.com/article/10.1007/s00371-013-0804-6/fulltext.html

[16] J. P. Rolland, M. W. Krueger, and A. A. Goon, "Dynamic focusing in head-mounted displays," pp. 463–470, 1999. [Online]. Available: http://dx.doi.org/10.1117/12.349412

[17] J. P. Rolland, R. L. Holloway, and H. Fuchs, "A comparison of optical and video se-through head-mounted displays," in Photonics for Industrial Applications, H. Das, Ed. International Society for Optics and Photonics, Dec. 1995, pp. 293–307. [Online]. Available: http://proceedings.spiedigitallibrary.org/proceeding.aspx?articleid=981546

[18] J. P. Rolland and H. Fuchs, "Optical Versus Video See-Through Head-Mounted Displays in Medical Visualization," Presence: Teleoperators and Virtual Environments, vol. 9, no. 3, pp. 287–309, Jun. 2000. [Online]. Available: http://www.mitpressjournals.org/doi/abs/10.1162/105474600566808#.VHdbWd_0-kA

[19] P. Milgram and F. Kishino, "A Taxonomy of Mixed Reality Visual Displays," IEICE TRANSACTIONS on Information and Systems, vol. E77-D, no. 12, pp. 1321–1329, Dec. 1994. [Online]. Available: http://search.ieice.org/bin/summary.php?id=e77-d_12_1321&category=D&year=1994&lang=E&abst=

[20] R. Azuma, "A survey of augmented reality," Presence: Teleoperators and Virtual Environments, vol. 6, no. 4, pp. 355–385, 1997. [Online]. Available: http://scholar.google.com/scholar?q=intitle:A+Survey+of+Augmented+Reality#0

[21] G. D. Love, D. M. Hoffman, P. J. W. Hands, J. Gao, A. K. Kirby, and M. S. Banks, "High-speed switchable lens enables the development of a volumetric stereoscopic display." Optics express, vol. 17, no. 18, pp. 15716–25, Aug. 2009. [Online]. Available: http://www.opticsexpress.org/abstract.cfm?URI=oe-17-18-15716

[22] J. P. Rolland and H. Hua, "Head-Mounted Display Systems," Encyclopedia of Optical Engineering, pp. 1–14, 2005. [Online]. Available: http://dx.doi.org/10.1081/E-EOE-120009801

[23] C. E. Rash, M. B. Russo, T. R. Letowski, and E. T. Schmeisser, "Helmet-mounted displays: Sensation, perception and cognition issues," DTIC Document, Tech. Rep., 2009.

[24] S. Shiwa, K. Omura, and F. Kishino, "Proposal for a 3D display with accommodative compensation: 3DDAC," Journal of the Society for Information Display, vol. 4, no. 4, pp. 255–261, Dec. 1996. [Online]. Available: http://onlinelibrary.wiley.com/doi/10.1889/1.1987395/abstract

[25] T. Takeda, Y. Fukui, K. Ikeda, and T. Iida, "Three-dimensional optometer III." Applied optics, vol. 32, no. 22, pp. 4155–68, Aug. 1993. [Online]. Available: http://www.ncbi.nlm.nih.gov/pubmed/20830060

[26] T. E. Lockhart and W. Shi, "Effects of age on dynamic accommodation." Ergonomics, vol. 53, no. 7, pp. 892–903, Jul. 2010. [Online]. Available: http://www.pubmedcentral.nih.gov/articlerender.fcgi?artid=2908311&tool=pmcentrez&rendertype=abstract

[27] N. Yanagisawa, K.-t. Kim, J.-Y. Son, T. Murata, and T. Orima, "Focus-distance-controlled 3D TV," in Photonics China '96, E. G. Lean, Z. Tian, and B. G. Wu, Eds. International Society for Optics and Photonics, Sep. 1996, pp. 120–125. [Online]. Available: http://proceedings.spiedigitallibrary.org/proceeding.aspx?articleid=1024409

[28] T. Shibata, T. Kawai, K. Ohta, M. Otsuki, N. Miyake, Y. Yoshihara, and T. Iwasaki, "Stereoscopic 3-D display with optical correction for the reduction of the discrepancy between accommodation and convergence," Journal of the Society for Information Display, vol. 13, no. 8, p. 665, 2005. [Online]. Available: http://doi.wiley.com/10.1889/1.1828693

[29] K. Ashizaki, M. Yamamoto, S. Miyaoka, and Sakuya Tamada, "Apparatus for direct display of an image on the retina of the eye using a scanning laser," Oct. 1994. [Online]. Available: http://www.google.com/patents/US5355181

[30] S. C. McQuaide, E. J. Seibel, J. P. Kelly, B. T. Schowengerdt, and T. A. Furness, "A retinal scanning display system that produces multiple focal planes with a deformable membrane mirror," Displays, vol. 24, no. 2, pp. 65–72, Aug. 2003. [Online]. Available: http://www.sciencedirect.com/science/article/pii/S0141938203000167

[31] B. T. Schowengerdt, E. J. Seibel, J. P. Kelly, N. L. Silverman, and T. A. Furness III, "Binocular retinal scanning laser display with integrated focus cues for ocular accommodation," in Electronic Imaging 2003. International Society for Optics and Photonics, May 2003, pp. 1–9. [Online]. Available: ftp://ftp.hitl.washington.edu/pub/publications/r-2006-35/r-2006-35.pdfhttp://proceedings.spiedigitallibrary.org/proceeding.aspx?articleid=755548

[32] B. T. Schowengerdt and E. J. Seibel, "True 3-D scanned voxel displays using single or multiple light sources," Journal of the Society for Information Display, vol. 14, no. 2, pp. 135–143, 2006.

[33] S. Suyama, M. Date, and H. Takada, "Three-Dimensional Display System with Dual-Frequency Liquid-Crystal Varifocal Lens," Japanese Journal of Applied Physics, vol. 39, no. Part 1, No. 2A, pp. 480–484, Feb. 2000. [Online]. Available: http://stacks.iop.org/1347-4065/39/i=2R/a=480

[34] S. Liu, D. Cheng, and H. Hua, "An optical see-through head mounted display with addressable focal planes," in 2008 7th IEEE/ACM International Symposium on Mixed and Augmented Reality. IEEE, Sep. 2008, pp. 33–42. [Online]. Available: http://ieeexplore.ieee.org/lpdocs/epic03/wrapper.htm?arnumber=4637321

[35] S. Liu and H. Hua, "Time-multiplexed dual-focal plane head-mounted display with a liquid lens," Optics Letters, vol. 34, no. 11, p. 1642, May 2009. [Online]. Available: http://www.opticsinfobase.org/viewmedia.cfm?uri=ol-34-11-1642&seq=0&html=true

[36] S. Liu, H. Hua, and D. Cheng, "A novel prototype for an optical see-through head-mounted display with addressable focus cues." IEEE transactions on visualization and computer graphics, vol. 16, no. 3, pp. 381–93, Jan. 2010. [Online]. Available: http://www.ncbi.nlm.nih.gov/pubmed/20224134

[37] M. Ye, B. Wang, and S. Sato, "Liquid-Crystal Lens with a Focal Length that is Variable in a Wide Range," Applied Optics, vol. 43, no. 35, p. 6407, 2004. [Online]. Available: http://ao.osa.org/abstract.cfm?URI=ao-43-35-6407

[38] G. Li, D. L. Mathine, P. Valley, P. Ayräs, J. N. Haddock, M. S. Giridhar, G. Williby, J. Schwiegerling, G. R. Meredith, B. Kippelen, S. Honkanen, and N. Peyghambarian, "Switchable electro-optic diffractive lens with high efficiency

for ophthalmic applications," Proceedings of the National Academy of Sciences of the United States of America, vol. 103, no. 16, pp. 6100–4, Apr. 2006. [Online]. Available: http://www.pubmedcentral.nih.gov/articlerender.fcgi?artid=1458838&tool=pmcentrez&rendertype=abstract

[39] J. Harrold, D. Wilkes, and G. Woodgate, "Switchable 2d/3d display–solid phase liquid crystal microlens array," in Proc. IDW, vol. 11, 2004, pp. 1495–1496.

[40] H.-k. Hong, S.-m. Jung, B.-j. Lee, H.-j. Im, and H.-h. Shin, "Autostereoscopic 2d/3d switching display using electric-field-driven lc lens (elc lens)," in SID Symposium Digest of Technical Papers, vol. 39, no. 1. Wiley Online Library, 2008, pp. 348–351.

[41] Y.-Y. Kao, Y.-P. Huang, K.-X. Yang, P. C.-P. Chao, C.-C. Tsai, and C.-N. Mo, "An auto-stereoscopic 3d display using tunable liquid crystal lens array that mimics effects of grin lenticular lens array," in SID symposium digest of technical papers, vol. 40, no. 1. Wiley Online Library, 2009, pp. 111–114.

[42] B. Lee and J.-H. Park, "Overview of 3d/2d switchable liquid crystal display technologies," in OPTO. International Society for Optics and Photonics, 2010, pp. 761 806–761 806.

[43] Y.-P. Huang, L.-Y. Liao, and C.-W. Chen, "2-d/3-d switchable autostereoscopic display with multi-electrically driven liquid-crystal (med-lc) lenses," Journal of the Society for Information Display, vol. 18, no. 9, pp. 642–646, 2010.

[44] S.-C. Liu, J.-F. Tu, C.-C. Gong, and C.-W. Chang, "Autostereoscopic 2-d/3-d display using a liquid crystal lens," in SID Symposium Digest of Technical Papers, vol. 41, no. 1. Wiley Online Library, 2010, pp. 432–435.

[45] Y.-P. Huang, C.-W. Chen, and Y.-C. Huang, "Superzone fresnel liquid crystal lens for temporal scanning auto-stereoscopic display," Display Technology, Journal of, vol. 8, no. 11, pp. 650–655, 2012.

[46] C.-W. Chen, Y.-P. Huang, and P.-C. Chen, "Dual direction overdriving method for accelerating 2d/3d switching time of liquid crystal lens on auto-stereoscopic display," Journal of Display Technology, vol. 8, no. 10, pp. 559–561, 2012.

[47] L. Lu, V. Sergan, T. Van Heugten, D. Duston, A. Bhowmik, and P. J. Bos, "Surface localized polymer aligned liquid crystal lens," Optics express, vol. 21, no. 6, pp. 7133–7138, 2013.

[48] J. P. Rolland, M. W. Krueger, and A. Goon, "Multifocal Planes Head-Mounted Displays," Applied Optics, vol. 39, no. 19, p. 3209, Jul. 2000. [Online]. Available: http://ao.osa.org/abstract.cfm?URI=ao-39-19-3209

[49] K. Akeley, S. J. Watt, A. R. Girshick, and M. S. Banks, "A stereo display prototype with multiple focal distances," in ACM SIGGRAPH 2004 Papers on - SIGGRAPH '04, vol. 23, no. 3. New York, New York, USA: ACM Press, Aug. 2004, p. 804. [Online]. Available: http://dl.acm.org/citation.cfm?id=1186562.1015804

[50] S. Liu and H. Hua, "A systematic method for designing depth-fused multi-focal plane three-dimensional displays." Optics express, vol. 18, no. 11, pp. 11 562–73, May 2010. [Online]. Available: http://www.opticsexpress.org/abstract.cfm?URI=oe-18-11-11562

[51] S. Ravikumar, K. Akeley, and M. S. Banks, "Creating effective focus cues in multi-plane 3D displays." Optics express, vol. 19, no. 21, pp. 20 940–52, Oct. 2011. [Online]. Available: http://www.opticsexpress.org/abstract.cfm?URI=oe-19-21-20940

[52] K. J. MacKenzie and S. J. Watt, "Eliminating accommodation-convergence conflicts in stereoscopic displays: Can multiple-focal-plane displays elicit continuous and consistent vergence and accommodation responses?" in IS&T/SPIE Electronic Imaging, A. J. Woods, N. S. Holliman, and N. A. Dodgson, Eds. International Society for Optics and Photonics, Feb. 2010, pp. 752 417–752 417–10. [Online]. Available: http://proceedings.spiedigitallibrary.org/proceeding.aspx?articleid=776088

[53] J. Rolland and K. Thompson, "Freeform optics: Evolution? No, revolution! — SPIE Newsroom: SPIE," SPIE Newsroom, 2012. [Online]. Available: http://spie.org/x88361.xml

[54] O. Cakmakci, A. Oranchak, and J. Rolland, "Dual-element off-axis eyeglass-based display," in Contract Proceedings 2006, G. G. Gregory, J. M. Howard, and R. J. Koshel, Eds.

[55] International Society for Optics and Photonics, Jun. 2006, pp. 63 420W–63 420W–7. [Online]. Available: http://proceedings.spiedigitallibrary.org/proceeding.aspx?articleid=1291750

[55] D. S. Bettinger, "Spectacle-mounted ocular display apparatus," Feb. 21 1989, uS Patent 4,806,011.

[56] O. Cakmakci and J. Rolland, "Design and fabrication of a dual-element off-axis near-eye optical magnifier," Optics Letters, vol. 32, no. 11, p. 1363, 2007. [Online]. Available: http://ol.osa.org/abstract.cfm?URI=ol-32-11-1363

[57] O. Cakmakci, B. Moore, H. Foroosh, and J. P. Rolland, "Optimal local shape description for rotationally non-symmetric optical surface design and analysis," Optics Express, vol. 16, no. 3, p. 1583, 2008. [Online]. Available: http://www.opticsexpress.org/abstract.cfm?URI=oe-16-3-1583

[58] O. Cakmakci, K. Thompson, P. Vallee, J. Cote, and J. P. Rolland, "Design of a free-form single-element head-worn display," in OPTO, L.-C. Chien, Ed. International Society for Optics and Photonics, Feb. 2010, pp. 761 803–761 803–6. [Online]. Available: http://proceedings.spiedigitallibrary.org/proceeding.aspx?articleid=747320

[59] I. Kaya, O. Cakmakci, K. Thompson, and J. P. Rolland, "The assessment of a stable radial basis function method to describe optical free-form surfaces," in Optical Fabrication and Testing. Optical Society of America, 2010, p. OTuD2.

[60] D. Cheng, Y. Wang, H. Hua, and J. Sasian, "Design of a wide-angle, lightweight head-mounted display using free-form optics tiling," Optics letters, vol. 36, no. 11, pp. 2098–100, Jun. 2011. [Online]. Available: http://ol.osa.org/abstract.cfm?URI=ol-36-11-2098

[61] Q. Wang, D. Cheng, Y. Wang, H. Hua, and G. Jin, "Design, tolerance, and fabrication of an optical see-through head-mounted display with free-form surface elements." Applied optics, vol. 52, no. 7, pp. C88–99, Mar. 2013. [Online]. Available: http://ao.osa.org/abstract.cfm?URI=ao-52-7-C88

[62] D. Cheng, Q. Wang, Y. Wang, and G. Jin, "Lightweight spatialy-multiplexed dual focal-plane head-mounted display using two freeform prisms," Chin. Opt. Lett., vol. 11, no. 3, pp. 031 201–, 2013. [Online]. Available: http://col.osa.org/abstract.cfm?URI=col-11-3-031201

[63] A. Maimone and H. Fuchs, "Computational augmented reality eyeglasses," in 2013 IEEE International Symposium on Mixed and Augmented Reality (ISMAR). IEEE, Oct. 2013, pp. 29–38. [Online]. Available: http://ieeexplore.ieee.org/lpdocs/epic03/wrapper.htm?arnumber=6671761

[64] D.-W. Kim, Y.-M. Kwon, Q.-H. Park, and S.-K. Kim, "Analysis of a head-mounted display-type multifocus display system using a laser scanning method," Optical Engineering, vol. 50, no. 3, p. 034006, Mar. 2011. [Online]. Available: http://opticalengineering.spiedigitallibrary.org/article.aspx?articleid=1157790

[65] X. Xiao, B. Javidi, M. Martinez-Corral, and A. Stern, "Advances in three-dimensional integral imaging: sensing, display, and applications [Invited]." Applied optics, vol. 52, no. 4, pp. 546–60, Feb. 2013. [Online]. Available: http://www.opticsinfobase.org/viewmedia.cfm?uri=ao-52-4-546&seq=0&html=true

[66] Y. Takaki, "Development of Super Multi-View Displays," ITE Transactions on Media Technology and Applications, vol. 2, no. 1, pp. 8–14, 2014. [Online]. Available: https://www.jstage.jst.go.jp/article/mta/2/1/2_8/_article

[67] D. Lanman and D. Luebke, "Near-eye light field displays," ACM Transactions on Graphics, vol. 32, no. 6, pp. 1–10, Nov. 2013. [Online]. Available: http://dl.acm.org/citation.cfm?id=2508363.2508366

[68] W. Song, Y. Wang, D. Cheng, and Y. Liu, "A high-resolution optical see-through head-mounted display with eyetracking capability." Chin. Opt. Lett., vol. 12, no. 6, pp. 060 010–, 2014. [Online]. Available: http://col.osa.org/abstract.cfm?URI=col-12-6-060010

[69] D. Lanman, M. Hirsch, Y. Kim, and R. Raskar, "Content-adaptive parallax barriers," in ACM SIGGRAPH Asia 2010 papers on - SIGGRAPH ASIA '10, vol. 29, no. 6. New York, New York, USA: ACM Press, Dec. 2010, p. 1. [Online]. Available: http://dl.acm.org/citation.cfm?id=1882262.1866164

[70] F. Heide, G. Wetzstein, R. Raskar, and W. Heidrich, "Adaptive image synthesis for compressive displays,"

*ACM Transactions on Graphics*, vol. 32, no. 4, p. 1, Jul. 2013. [Online]. Available: http://dl.acm.org/citation.cfm?id=2461912.2461925

[71] A. Maimone, D. Lanman, K. Rathinavel, K. Keller, D. Luebke, and H. Fuchs, "Pinlight displays: Wide Field of View Augmented Reality Eyeglasses using Defocused Point Light Sources," in *ACM SIGGRAPH 2014 Emerging Technologies on - SIGGRAPH '14*. New York, New York, USA: ACM Press, Jul. 2014, pp. 1–1. [Online]. Available: http://dl.acm.org/citation.cfm?id=2614066.2614080

[72] H. Hua and C. Gao, "A compact eyetracked optical see-through head-mounted display," in *IS&T/SPIE Electronic Imaging*, A. J. Woods, N. S. Holliman, and G. E. Favalora, Eds. International Society for Optics and Photonics, Feb. 2012, p. 82881F. [Online]. Available: http://proceedings.spiedigitallibrary.org/proceeding.aspx?articleid=1282686

[73] H. Hua, X. Hu, and C. Gao, "A high-resolution optical see-through head-mounted display with eyetracking capability." *Optics express*, vol. 21, no. 25, pp. 30 993–8, Dec. 2013. [Online]. Available: http://www.opticsinfobase.org/viewmedia.cfm?uri=oe-21-25-30993&seq=0&html=true

[74] G. Beach, C. Cohen, J. Braun, and G. Moody, "Eye tracker system for use with head mounted displays," in *SMC'98 Conference Proceedings. 1998 IEEE International Conference on Systems, Man, and Cybernetics (Cat. No.98CH36218)*, vol. 5. IEEE, 1998, pp. 4348–4352. [Online]. Available: http://ieeexplore.ieee.org/lpdocs/epic03/wrapper.htm?arnumber=727531

[75] A. T. Duchowski, E. Medlin, A. Gramopadhye, B. Melloy, and S. Nair, "Binocular eye tracking in VR for visual inspection training," in *Proceedings of the ACM symposium on Virtual reality software and technology - VRST '01*. New York, New York, USA: ACM Press, Nov. 2001, p. 1. [Online]. Available: http://dl.acm.org/citation.cfm?id=505008.505010

[76] L. Vaissie and J. Rolland, "Eyetracking in head-mounted displays: analysis and design," Technical Report TR98-007, University of Central Florida, Tech. Rep., 1998.

[77] ——, "Head mounted display with eyetracking capability," Aug. 2002. [Online]. Available: http://www.google.com/patents/US6433760

[78] L. Vaissie, J. P. Rolland, and G. M. Bochenek, "Analysis of eyepoint locations and accuracy of rendered depth in binocular head-mounted displays," in *Electronic Imaging '99*, J. O. Merritt, M. T. Bolas, and S. S. Fisher, Eds. International Society for Optics and Photonics, May 1999, pp. 57–64. [Online]. Available: http://proceedings.spiedigitallibrary.org/proceeding.aspx?articleid=978731

[79] H. Hua, "Integration of eye tracking capability into optical see-through head-mounted displays," in *Photonics West 2001 - Electronic Imaging*, A. J. Woods, M. T. Bolas, J. O. Merritt, and S. A. Benton, Eds. International Society for Optics and Photonics, Jun. 2001, pp. 496–503. [Online]. Available: http://proceedings.spiedigitallibrary.org/proceeding.aspx?articleid=903622

[80] C. Curatu, H. Hua, and J. Rolland, "Projection-based head-mounted display with eye tracking capabilities," in *Optics & Photonics 2005*, J. M. Sasian, R. J. Koshel, and R. C. Juergens, Eds. International Society for Optics and Photonics, Aug. 2005, pp. 58 750J–58 750J–9. [Online]. Available: http://proceedings.spiedigitallibrary.org/proceeding.aspx?articleid=1282664

[81] H. Hua, P. Krishnaswamy, and J. P. Rolland, "Video-based eyetracking methods and algorithms in head-mounted displays," *Optics Express*, vol. 14, no. 10, p. 4328, 2006. [Online]. Available: http://www.opticsexpress.org/abstract.cfm?URI=oe-14-10-4328

[82] H. Hua, C. W. Pansing, and J. P. Rolland, "Modeling of an eye-imaging system for optimizing illumination schemes in an eye-tracked head-mounted display," *Applied Optics*, vol. 46, no. 31, p. 7757, 2007. [Online]. Available: http://ao.osa.org/abstract.cfm?URI=ao-46-31-7757

[83] Y. David, B. Apter, N. Thirer, I. Baal-Zedaka, and U. Efron, "Design of integrated eye tracker-display device for head mounted systems," in *SPIE Photonic Devices + Applications*, E. L. Dereniak, J. P. Hartke, P. D. LeVan, R. E. Longshore, and A. K. Sood, Eds. International Society for Optics and Photonics, Aug. 2009, pp. 741 910–741 910–10. [Online]. Available: http://proceedings.spiedigitallibrary.org/proceeding.aspx?articleid=785356

[84] X. Hu and H. Hua, "Optical Design of An Eyetracked Head-mounted Display using Freeform Waveguide," in *Classical Optics 2014*. Washington, D.C.: OSA, 2014, p. ITh3A.4. [Online]. Available: http://www.opticsinfobase.org/abstract.cfm?URI=IODC-2014-ITh3A.4

[85] M. Vinnikov and R. S. Allison, "Gaze-contingent depth of field in realistic scenes," in *Proceedings of the Symposium on Eye Tracking Research and Applications - ETRA '14*. New York, New York, USA: ACM Press, Mar. 2014, pp. 119–126. [Online]. Available: http://dl.acm.org/citation.cfm?id=2578153.2578170

[86] M. Day, D. Seidel, L. S. Gray, and N. C. Strang, "The effect of modulating ocular depth of focus upon accommodation microfluctuations in myopic and emmetropic subjects." *Vision research*, vol. 49, no. 2, pp. 211–8, Jan. 2009. [Online]. Available: http://www.sciencedirect.com/science/article/pii/S0042698908005117

[87] L. O'Hare, T. Zhang, H. T. Nefs, and P. B. Hibbard, "Visual discomfort and depth-of-field." *i-Perception*, vol. 4, no. 3, pp. 156–69, Jan. 2013. [Online]. Available: http://www.pubmedcentral.nih.gov/articlerender.fcgi?artid=3690407&tool=pmcentrez&rendertype=abstract

[88] A. State, J. Ackerman, G. Hirota, J. Lee, and H. Fuchs, "Dynamic virtual convergence for video see-through head-mounted displays: maintaining maximum stereo overlap throughout a close-range work space," in *Proceedings IEEE and ACM International Symposium on Augmented Reality*, 2001, pp. 137 – 146.

[89] A. Sherstyuk, A. Dey, C. Sandor, and A. State, "Dynamic eye convergence for head-mounted displays improves user performance in virtual environments," in *Proceedings of the ACM SIGGRAPH Symposium on Interactive 3D Graphics and Games - I3D '12*. New York, New York, USA: ACM Press, Mar. 2012, p. 23. [Online]. Available: http://dl.acm.org/citation.cfm?id=2159616.2159620

[90] M. Fisker, K. Gram, K. K. Thomsen, D. Vasilarou, and M. Kraus, "Automatic Convergence Adjustment in Stereoscopy Using Eye Tracking," in *EG 2013 - Posters*, 2013, pp. 23– 24.

[91] M. Bernhard, C. Dell'mour, M. Hecher, E. Stavrakis, and M. Wimmer, "The effects of fast disparity adjustment in gaze-controlled stereoscopic applications," *Proceedings of the Symposium on Eye Tracking Research and Applications - ETRA '14*, pp. 111–118, 2014. [Online]. Available: http://dl.acm.org/citation.cfm?doid=2578153.2578169

[92] J.-S. Lee, L. Goldmann, and T. Ebrahimi, "Paired comparison-based subjective quality assessment of stereoscopic images," *Multimedia tools and applications*, vol. 67, no. 1, pp. 31–48, 2013.

[93] R. M. Groves, F. J. Fowler Jr, M. P. Couper, J. M. Lepkowski, E. Singer, and R. Tourangeau, *Survey methodology*. John Wiley & Sons, 2013.

[94] W. Wesemann and B. Dick, "Accuracy and accommodation capability of a handheld autorefractor," *Journal of Cataract & Refractive Surgery*, vol. 26, no. 1, pp. 62–70, 2000.

[95] T. Dave, "Automated refraction: design and applications," *Optom Today*, vol. 48, pp. 28–32, 2004.

[96] Y. Takaki, "High-Density Directional Display for Generating Natural Three-Dimensional Images," *Proceedings of the IEEE*, vol. 94, no. 3, pp. 654–663, Mar. 2006. [Online]. Available: http://ieeexplore.ieee.org/lpdocs/epic03/wrapper.htm?arnumber=1605209

[97] R. Suryakumar, J. P. Meyers, E. L. Irving, and W. R. Bobier, "Application of video-based technology for the simultaneous measurement of accommodation and vergence." *Vision research*, vol. 47, no. 2, pp. 260–8, Jan. 2007. [Online]. Available: http://www.sciencedirect.com/science/article/pii/S0042698906004767

[98] H. Heo, W. O. Lee, K. Y. Shin, and K. R. Park, "Quantitative measurement of eyestrain on 3D stereoscopic display considering the eye foveation model and edge information." *Sensors (Basel, Switzerland)*, vol. 14, no. 5, pp. 8577–604, Jan. 2014. [Online]. Available: http://www.pubmedcentral.nih.gov/articlerender.fcgi?artid=4063008&tool=pmcentrez&rendertype=abstract

[99] H. Oyamada, A. Iijima, A. Tanaka, K. Ukai, H. Toda, N. Sugita, M. Yoshizawa, and T. Bando, "A pilot study on pupillary and cardiovascular changes induced by stereoscopic video movies." Journal of neuroengineering and rehabilitation, vol. 4, no. 1, p. 37, Jan. 2007. [Online]. Available: http://www.jneuroengrehab.com/content/4/1/37

[100] C. J. Kim, S. Park, M. J. Won, M. Whang, and E. C. Lee, "Autonomic nervous system responses can reveal visual fatigue induced by 3D displays." Sensors (Basel, Switzerland), vol. 13, no. 10, pp. 13 054–62, Jan. 2013. [Online]. Available: http://www.pubmedcentral.nih.gov/articlerender.fcgi?artid=3859049&tool=pmcentrez&rendertype=abstract

[101] S. Mun, M.-C. Park, S. Park, and M. Whang, "SSVEP and ERP measurement of cognitive fatigue caused by stereoscopic 3D." Neuroscience letters, vol. 525, no. 2, pp. 89–94, Sep. 2012. [Online]. Available: http://www.sciencedirect.com/science/article/pii/S0304394012010105

[102] H. Hagura and M. Nakajima, "Study of asthenopia caused by the viewing of stereoscopic images: measurement by MEG and other devices," in Electronic Imaging 2006, B. E. Rogowitz, T. N. Pappas, and S. J. Daly, Eds. International Society for Optics and Photonics, Feb. 2006, pp. 60 570K–60 570K–11. [Online]. Available: http://proceedings.spiedigitallibrary.org/proceeding.aspx?articleid=727891

[103] J. Frey, L. Pommereau, F. Lotte, and M. Hachet, "Assessing the zone of comfort in stereoscopic displays using EEG," in Proceedings of the extended abstracts of the 32nd annual ACM conference on Human factors in computing systems - CHI EA '14. New York, New York, USA: ACM Press, Apr. 2014, pp. 2041–2046. [Online]. Available: http://dl.acm.org/citation.cfm?id=2559206.2581191

[104] E. Hecht, "Optics 4th edition," Optics, 4th Edition, Addison Wesley Longman Inc, 1998, vol. 1, 1998.